Molecular Microbiology (2013) 87(6), 1183–1199 ■
doi:10.1111/mmi.12158
First published online 6 February 2013

Interplay between predicted inner-rod and gatekeeper in controlling substrate specificity of the type III secretion system

Youness Cherradi,[1] Lionel Schiavolin,[1] Simon Moussa,[1] Alaeddine Meghraoui,[1] Ahmed Meksem,[1] Latéfa Biskri,[1] Mohamed Azarkan,[2] Abdelmounaaïm Allaoui[1*†] and Anne Botteaux[1†]
[1]*Laboratoire de Bactériologie Moléculaire and* [2]*Protein Chemistry Unit, Faculté de Médecine, Université Libre de Bruxelles, Route de Lennik, 808, 1070, Bruxelles, Belgium.*

Summary

The type III secretion apparatus (T3SA) is a multi-protein complex central to the virulence of many Gram-negative pathogens. Currently, the mechanisms controlling the hierarchical addressing of needle subunits, translocators and effectors to the T3SA are still poorly understood. In *Shigella,* MxiC is known to sequester effectors within the cytoplasm prior to receiving the activation signal from the needle. However, molecules involved in linking the needle and MxiC are unknown. Here, we demonstrate a molecular interaction between MxiC and the predicted inner-rod component MxiI suggesting that this complex plugs the T3SA entry gate. Our results suggest that MxiI–MxiC complex dissociation facilitates the switch in secretion from translocators to effectors. We identified MxiC^{F206S} variant, unable to interact with MxiI, which exhibits a constitutive secretion phenotype although it remains responsive to induction. Moreover, we identified the *mxiI*^{Q67A} mutant that only secretes translocators, a phenotype that was suppressed by coexpression of the MxiC^{F206S} variant. We demonstrated the interaction between MxiI and MxiC homologues in *Yersinia* and *Salmonella*. Lastly, we identified an interaction between MxiC and chaperone IpgC which contributes to understanding how translocators secretion is regulated. In summary, this study suggests the existence of a widely conserved T3S mechanism that regulates effectors secretion.

Accepted 15 January, 2013. *For correspondence. E-mail aallaoui@ulb.ac.be; Tel. (+32) 25556251; Fax (+32) 25556116. †Co-last authors.

Introduction

Type 3 secretion systems (T3SSs) are macromolecular complexes of many Gram-negative bacteria and are crucial factors for their virulence capabilities. They are composed of at least 21 distinct proteins forming three major components: a transmembrane region, a cytoplasmic bulb also called C-ring, and an extracellular needle through which bacteria can inject its proteins into the host cells (Cornelis, 2006). This multi-protein complex is also comprised of a membrane-associated ATPase which faces the bacterial cytoplasm thought to be involved in facilitating the entry of export substrates into the T3SA channel (Akeda and Galan, 2005; Lara-Tejero *et al.*, 2011).

In contrast to the T3SA structural components, the injected effectors are highly diversified and possess multiple mechanisms to hijack numerous cellular pathways of the host cell leading to bacterial establishment. For example, some effectors can induce cytoskeleton reorganization to promote bacterial entry (Patel and Galan, 2005; Parsot, 2009), others act as immune modulators to avoid host defences (Espinosa and Alfano, 2004; Ogawa *et al.*, 2008) or phagocytosis by macrophages (Shao, 2008). One of the most important properties of this secretion system is the ability to adapt rapidly to host cell contact in a well-organized manner to achieve effective virulence (Deane *et al.*, 2010; Buttner, 2012). First, T3SA inserts hydrophobic proteins, also called translocators, into the cell membrane to form a pore through which effector proteins are injected into the host cell. In the absence of signal from host cell, the T3SA is inactive and is plugged by the tip complex proteins (Blocker *et al.*, 2008).

Among bacteria that use a T3SA, *Shigella* causes the most devastating epidemics of bacterial infection in the developing world with up to one million deaths each year, essentially among young children (Kotloff *et al.*, 1999). *Shigella* uses the T3SA to penetrate enterocytes and to disseminate into the colonic epithelium leading to a partial destruction of the mucosal lining and shigellosis symptoms. Most of the virulence factors of *Shigella* are encoded by a large virulence plasmid harbouring a 31 kb region that is sufficient to promote bacterial entry into host cells (Buchrieser *et al.*, 2000). The 'entry' region is organized in

two loci, one encoding Mxi-Spa proteins that form the T3SA and the other encoding early substrates of this apparatus and their cognate chaperones. At 37°C, the needle subunit, MxiH and the predicted inner-rod component MxiI are secreted through the T3SA base, then MxiH polymerizes to form up to 50 nm needle (Magdalena *et al*., 2002). MxiI is homologue to proteins forming the inner rod in other bacteria including PrgJ of *Salmonella,* YscI of *Yersinia* and PscI of *Pseudomonas* (Blocker *et al*., 2001; Marlovits *et al*., 2004; 2006). Once the needle length has reached 50 nm, it is plugged by the tip complex composed of IpaB and IpaD in the absence of T3S induction and before host cell contact. Exposure of IpaD at the tip serves, with IpaB, as sensors of the host cell contact (Olive *et al*., 2007; Veenendaal *et al*., 2007). After the cell contact is sensed by this tip, IpaC is secreted to form with IpaB, a translocation pore in the host cell membrane. At this stage, another set of IpaB/IpaC and early effectors accumulate within the bacterial cytoplasm and bind to their respective chaperone, such as IpgC for the translocators. Once *Shigella* comes into contact with the host cell membrane, T3SA activation by an uncharacterized signal leads to the insertion of IpaB and IpaC into the host membrane and enhances translocators/effectors secretion. The resulting pore, also called the translocon, serves as a gate for secreted effectors to gain access to host cytoplasm. Moreover, the expression of a set of 'late' effectors, acting at later stage of infection, is controlled by the T3SA activity (Mavris *et al*., 2002). In the absence of cell contact, their expression is turned off by OspD1, a protein sequestering the transcriptional activator MxiE that requires the IpgC cofactor for activation of late effectors gene transcription (Parsot *et al*., 2005). Upon IpaB, IpaC and OspD1 secretion, released IpgC binds to MxiE leading to activation of late effectors genes transcription (Parsot *et al*., 2005; Pilonieta and Munson, 2008).

In *Shigella* tip complex mutants (*ipaB, ipaD*), the translocators, early and late effectors are constitutively secreted (Menard *et al*., 1994; Parsot *et al*., 1995). This suggests that the activation signal (cell contact) in these mutants is already transmitted to the T3SA base. Interestingly, similar findings were described for the *mxiC* mutant although the tip complex was still present suggesting the existence of a mechanism that retains them inside bacteria prior to cell contact. Moreover, the translocators secretion is known to be impaired in response to Congo red (CR) (Botteaux *et al*., 2009; Martinez-Argudo and Blocker, 2010), an amphipathic dye used to mimic host cell contact (Bahrani *et al*., 1997). MxiC shares its function with the other members of the YopN family including YopN (*Yersinia enterocolitica*), InvE (*Salmonella enterica*), SepL [enterohaemorrhagic (EHEC) and enteropathogenic (EPEC) *Escherichia coli*], HrpJ (*Pseudomonas syringae*) and PopN (*Pseudomonas aeruginosa*) (Pallen *et al*., 2005). The MxiC crystal structure reveals three distinct 'X-bundle' structures made of four, five and four α-helices respectively (Deane *et al*., 2008). A recent study also highlighted the role of MxiC in the activation signal transmission from T3SA tip to the base whereby *mxiH*^{K69A} and *mxiH*^{R83A} mutants are unable to promote effectors and MxiC secretion (Kenjale *et al*., 2005; Martinez-Argudo and Blocker, 2010). Interestingly, this defect was abrogated in these mutants through *mxiC* gene inactivation, suggesting that MxiC secretion is a prerequisite for effectors secretion upon T3S induction.

How the activation signal is transmitted and leads to effectors secretion remains a matter of debate. The most highly supported model, called 'allosteric model', attempted to highlight the needle role in signal transmission. Some *mxiH* mutants, such as *mxiH*^{K69A}, *mxiH*^{R83A}, *mxiH*^{P44A} and *mxiH*^{Q51A}, are known to affect secretion of effectors through a variety of mechanisms (Kenjale *et al*., 2005). It was suggested that the signal is first sensed by the tip complex and transmitted along the needle, thereby reaching the base and promoting effectors secretion. MxiC is considered as a strong signal receiver candidate but the components facilitating the interaction between MxiC and the needle remain unknown.

In the present study, we identified one of these missing elements as the predicted inner-rod component MxiI. We revealed an important biological insight based on MxiI and MxiC interaction and highlighted its role in sequestering effectors prior to T3S induction. We have also shown that the molecular interaction between MxiI and MxiC homologues is common in other bacterial species, leading us to suggest the existence of a shared mechanism that regulates the switch to effectors secretion. Furthermore, we generated the *mxiI*^{Q67A} mutant and showed that it exhibits almost the *mxiH*^{K69A} effector mutant phenotype. Interestingly, effectors secretion was restored in this strain by a suppressive *mxiC*^{F206S} extragenic mutation. Lastly, we put forward evidence suggesting the role of a newly identified interaction between MxiC and the chaperone IpgC in the regulation of translocators secretion.

Results

Mutational analysis revealed the MxiC^{F206S} *variant that discriminates between constitutive and inducible secretion states*

While wild-type *Shigella* secretes only low levels of Ipa proteins, *mxiC* mutant exhibits a constitutive secretion of effectors (Botteaux *et al*., 2009). Ferracci *et al*. (2005) showed that residues clustered in the central region of YopN are important for secretion. Such region corresponds to X-bundle 2 of MxiC, which is spatially separated from the SycN/YscB-binding domain of YopN (residues 81–160,

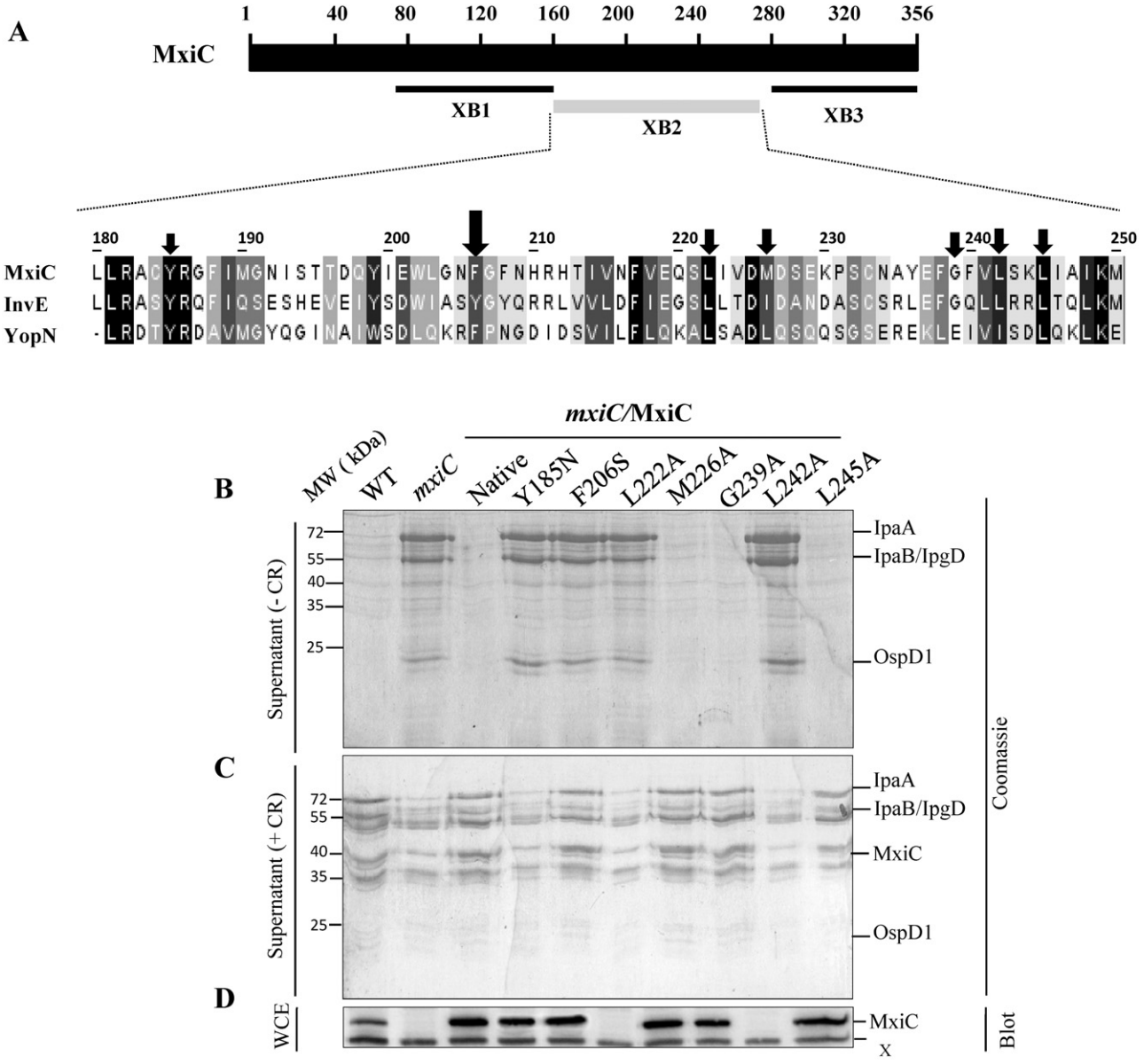

Fig. 1. MxiC^{F206S} does not control effectors secretion but restores the CR responsiveness.
A. Schematic representation of the MxiC's organization domains and sequences alignment of MxiC (*Shigella*), InvE (*Salmonella*) and YopN (*Yersinia*) using CLUSTALW2 and Jalview programs. Residues are boxed in black (identity) and grey scale (similarity score). The black vertical arrows point to the seven MxiC residues mutated in this study.
B and C. Culture supernatants of strains: wild-type M90T (WT), *mxiC* mutant (*mxiC*), *mxiC* mutant complemented by pSU18-MxiC or its seven mutated derivatives, not induced with Congo red (– CR) (B) or induced during 10 min (+ CR) (C) were resolved by SDS-PAGE and analysed by Coomassie blue staining.
D. Analysis of MxiC and its derivatives production by Western blot using anti-MxiC polyclonal antibodies.
E–H. Proteins from the supernatant of wild-type M90T (WT), *mxiC* mutant (*mxiC*), *mxiC*/pSU18-MxiC, or *mxiC*/pSU18-MxiC^{F206S} induced (+ CR) (E, F) or not (– CR) (G, H) were resolved by SDS-PAGE either stained with Coomassie blue (E, G) or analysed by Western blot (F, H) using antibodies directed against IpaB, OspD1, MxiC, IpaA or IpaH.
I. Analysis of proteins production by Western blot using the same antibodies.
Shown data are representative of three independent experiments.

X-bundle 1) and from the region homologue to TyeA (residues 271–356, X-bundle 3) (Day and Plano, 1998; Pallen *et al.*, 2005; Joseph and Plano, 2007) (Fig. 1A). In other bacterial species, the structural and sequence alignment analysis point towards highly conserved residues between MxiC and its homologues. In support of this, mutations of conserved residues in the interfaces between YopN domains, such as Y202 to an Asparagine, constitutively

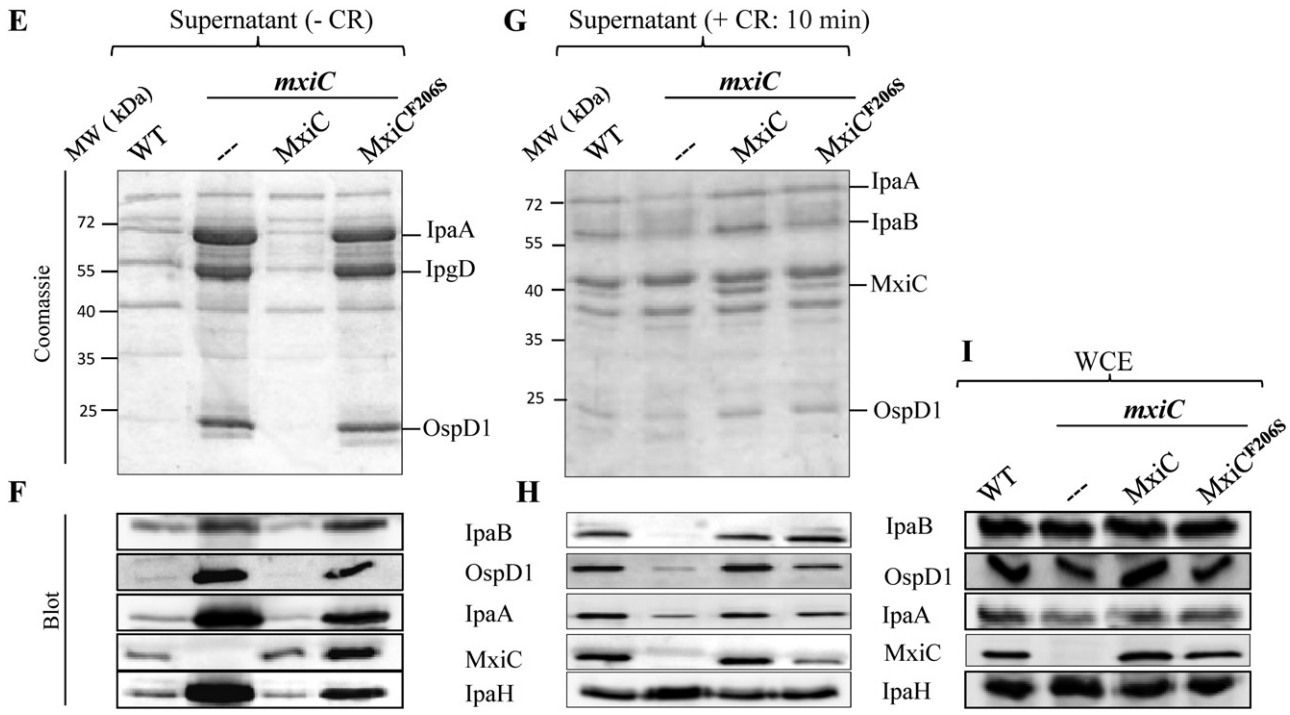

Fig. 1. *cont.*

block Yop secretion (Ferracci *et al.*, 2005). Interestingly, Deane *et al.* (2008) suggested that the hydrophobic patch on the surface of MxiC central domain (X-bundle 2) consisting of residues Leu222, Met226, Gly239, Leu242 and Leu245 interacts with other T3S components (Fig. 1A). Thus, to gain further insights into the mechanism by which MxiC regulates secretion, we generated point mutations on the pAB108′ (pSU18-*mxiC*) of the five residues described above and mutated residue Y185 corresponding to YopN^{Y202}. Additionally, we mutated F206 to a Serine as this residue is conserved in YopN (Fig. 1A). We subsequently analysed proteins secreted by the *mxiC* mutant expressing generated variants (Y185N, F206S, L222A, M226A, G239A, L242A and L245A) under both constitutive and CR inducible secretion conditions (Fig. 1B and C). When bacteria are growing in broth, the T3SA is weakly active and translocators and effectors are stored in the cytoplasm in association with their dedicated chaperones. The activation of the T3SA upon contact with epithelial cells or exposure to the dye Congo red (Parsot *et al.*, 1995; Bahrani *et al.*, 1997) leads to increased transcription of 12 effector-encoding genes scattered on the virulence plasmid, including members of the *ipaH* family (Demers *et al.*, 1998). While MxiC^{M226A}, MxiC^{G239A} and MxiC^{L245A} were able to restore wild-type secretion, the MxiC^{L222A}, MxiC^{L242A} and MxiC^{Y185N} exhibited the *mxiC* mutant phenotype since they were unable neither to control effectors secretion nor to respond to CR induction (Fig. 1B and C). Interestingly, the *mxiC^{F206S}* variant presented a new and unexpected phenotype discriminating between constitutive and CR induction states (Fig. 1B and C). The constitutive expression of the seven MxiC variants from the p*lac* promoter was assessed by Western blot analysis using anti-MxiC rabbit polyclonal antibodies (Fig. 1D). Out of the seven generated variants, MxiC^{L222A} and MxiC^{L242A} were not detectable (Fig. 1D) which explain the lack of secretion control by these two variants (Fig. 1B and C).

Next, we focused our study on the newly identified phenotype expressed by the *mxiC^{F206S}* mutation. In the absence of T3S induction, MxiC^{F206S} gave rise to a constitutive secretion of effectors IpaA and IpaH (Fig. 1E and F). In contrast, upon T3S induction with CR for 10 min, MxiC^{F206S} fully restored wild-type secretion of IpaB, OspD1, as well as effectors IpaA and IpaH (Fig. 1G and H). As MxiC is itself a T3S substrate, compared with native MxiC, we found that secretion of MxiC^{F206S}, although produced at wild-type level, was reduced under CR induction (Fig. 1H). This phenotype could be due to the increased secretion of MxiC^{F206S} seen in the absence of induction (Fig. 1F). Hence, the observed effect on secretion was not due to the lack of proteins production (Fig. 1I).

MxiC folding is not impaired by the F206S single mutation

One possible explanation regarding the phenotype associated with the *mxiC^{F206S}* mutation could be the misfolding of MxiC^{F206S}. To test this hypothesis, highly purified His-

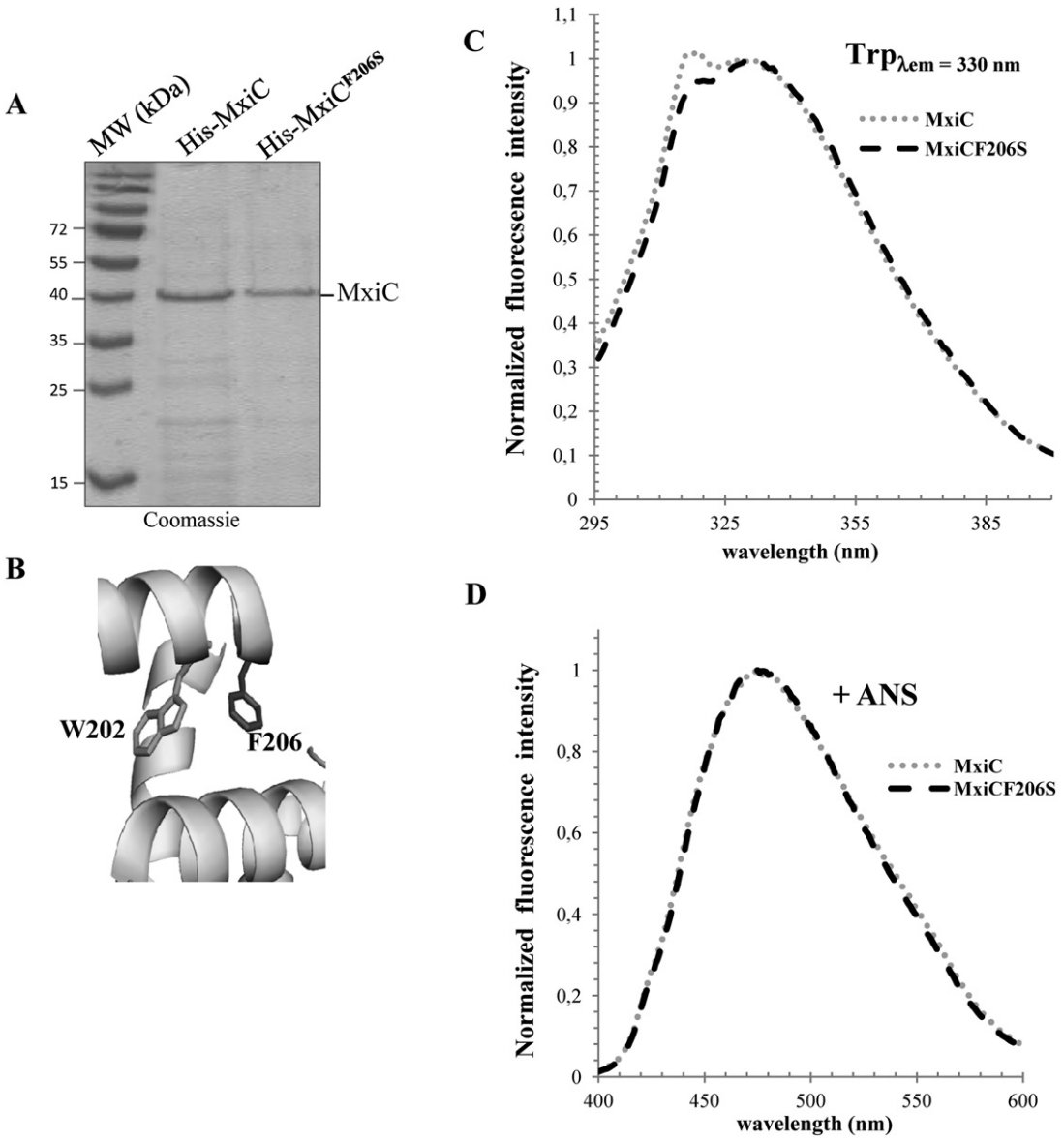

Fig. 2. His-MxiC and His-MxiC^{F206S} adopt the same overall protein fold.
A. Aliquots (~ 10 μg) of purified His-MxiC or His-MxiC^{F206S} after gel filtration chromatography were resolved by SDS-PAGE and stained with Coomassie blue.
B. Cartoon representation, obtained from the crystal structure data of MxiC (PDB ID code 2VJ5), of Trp202 and Phe206 showing their close proximity.
C. Normalized and corrected tryptophan fluorescence spectra of His-MxiC and His-MxiC^{F206S}.
D. Normalized and corrected extrinsic fluorescence spectra of His-MxiC and His-MxiC^{F206S} in the presence of ANS.

MxiC and His-MxiC^{F206S} (Fig. 2A) were assessed in two fluorescence assays (see *Experimental procedures*). The usefulness of fluorescence spectroscopy, as a valid tool to monitor possible structural changes in His-MxiC^{F206S} protein upon the single mutation, was based on available MxiC crystallographic data (Deane *et al*., 2008) and the presence of a single Tryptophan (W202) located in close proximity to residue F206 (Fig. 2B). It is thus reasonable to assume that if some structural modification could occur, the Tryptophan fluorescence will be also affected by its environment changes. As shown in Fig. 2C, the intrinsic fluorescence spectrum of purified His-MxiC^{F206S} is quite superimposable on that of unmodified His-MxiC. In addition, the fluorescence peak occurred at around 330 nm, demonstrating that the aromatic residues are located in an apolar environment as a result of the native and compact conformation adopted by the two protein forms, at least around the mutated domain.

The second method used to assess protein folding was based on the ANS binding assay (See *Experimental*

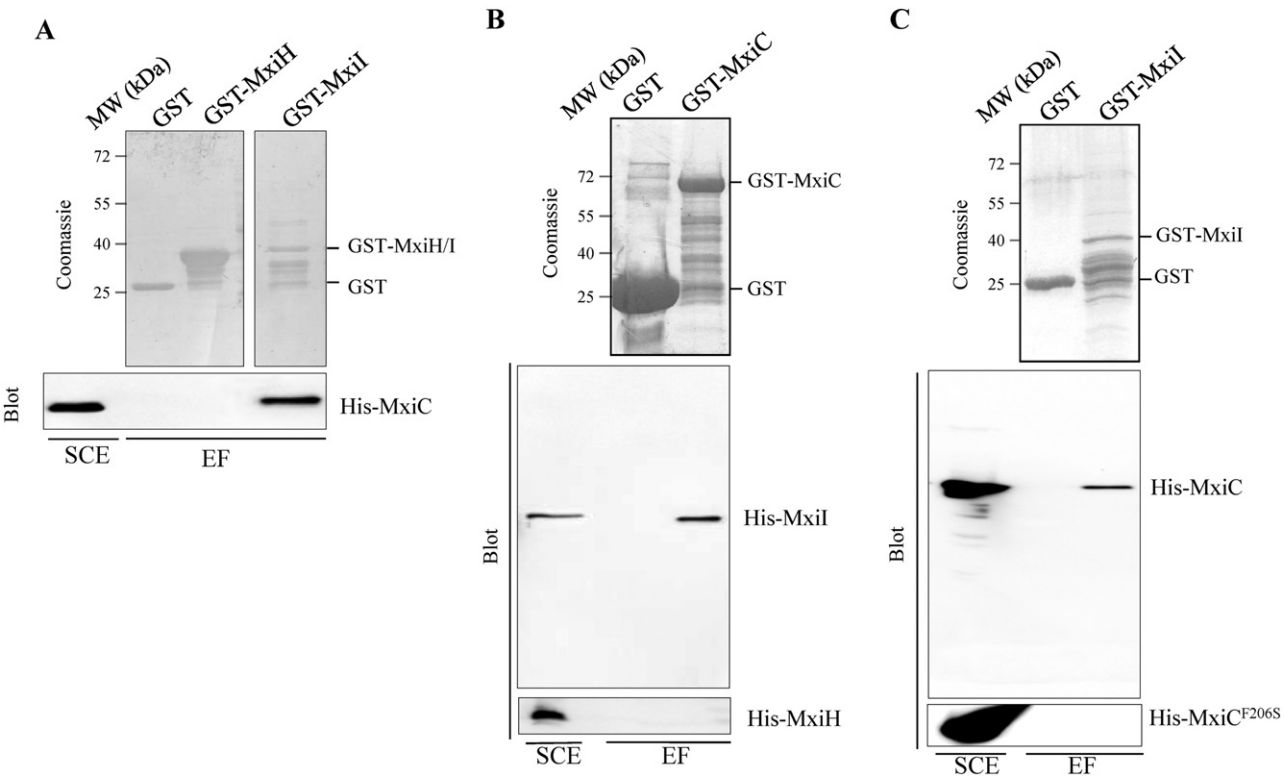

Fig. 3. MxiC interacts with the inner-rod component, MxiI.
A. Soluble cell extract (SCE) of *E. coli* producing His-MxiC was incubated with GST-MxiH, GST-MxiI or GST alone bound to gluthatione-Sepharose.
B. SCEs of *E. coli* producing His-MxiI or His-MxiH were incubated with GST-MxiC or GST alone bound to gluthatione-Sepharose.
C. SCEs of *E. coli* producing His-MxiC or His-MxiC^{F206S} were incubated with GST-MxiI or GST alone bound to gluthatione-Sepharose.
Eluted fractions (EF) with reduced glutathione were resolved on SDS-PAGE and analysed by Coomassie blue staining or by Western blot using an anti-His mAb. The binding assay was repeated at least three times.

procedures). The incubation of purified His-MxiC or His-MxiC^{F206S} with a large excess of ANS showed the same behaviour of the two proteins, resulting in an increase in the fluorescence intensity and a blue shifting of its λmax, demonstrating some dye binding to the two proteins (Fig. 2D). On a quantitative point of view, the fluorescence intensity reached in the presence of the two proteins is quite comparable. ANS binding can be partly explained by the fact that the first 70–80 residues of MxiC were reported to be poorly structured and consequently not characterized by a well-defined electron density. Furthermore, it was suggested that MxiC does not possess a globular structure and/or be partially disordered (Deane *et al.*, 2008), probably explaining the ANS binding characteristics. Taking together, our results suggest that the folding of His-MxiC^{F206S} is not affected by the single mutation and adopts the same overall conformation as His-MxiC.

MxiC interacts with the predicted inner-rod protein MxiI

It was reported that some specific *mxiH* mutants affect MxiC secretion in response to CR induction and thereby inhibiting the secretion of effectors. Hence, the signal leading to effector secretion is thought to be transmitted to MxiC via needle subunits (Martinez-Argudo and Blocker, 2010). Subsequently, we investigated potential direct interaction between MxiC, MxiH and MxiI. To do so, we constructed three plasmids encoding GST-MxiI, GST-MxiH and His-MxiC and performed GST pull-down assay (see *Experimental procedure*). Bacterial lysates containing His-MxiC were incubated with glutathione-Sepharose beads pre-coated with GST-MxiI, GST-MxiH or GST alone. We revealed an interaction between MxiC and MxiI, while no interaction was detected between MxiC and MxiH or GST alone (Fig. 3A). Besides, the MxiC–MxiI interaction was detected in *E. coli* suggesting that no additional T3S components are required.

As the molecular weight of GST is 28 kDa and the one of MxiH does not exceed 9 kDa, we cannot exclude the possibility that GST itself may prevent MxiH interaction with MxiC by some steric hindrance effect. To overcome such experimental artefact, we produced His-MxiH and tested it for GST-MxiC interaction. As a positive control, we also incubated GST-MxiC with His-MxiI. The obtained results

confirmed that MxiI, but not MxiH, interacts with MxiC (Fig. 3B).

Since the MxiC^{F206S} variant does not control secretion of effectors under non-inducible secretion condition but is still able to respond to CR induction, we assessed MxiC^{F206S} interaction with MxiI. For that purpose, we generated the His-MxiC^{F206S} variant and performed a GST-MxiI pull-down assay. In contrast to unmodified His-MxiC, His-MxiC^{F206S} was not co-eluted with GST-MxiI although produced at wild-type level (Fig. 3C). This finding suggests that the interaction between MxiC and MxiI may sequester effectors prior to T3S induction.

MxiC–MxiI complex dissociation is presumably required to recover effectors secretion in the mxiH^{K69A} background

Needle subunit *mxiH* mutants (*mxiH^{K69A}* and *mxiH^{R83A}*) were defined as 'effector mutants' since they secrete translocators upon CR induction, but are unable to secrete MxiC and effector proteins. This defect was suppressed upon *mxiC* gene inactivation in these mutants (Kenjale *et al*., 2005; Martinez-Argudo and Blocker, 2010). Such a finding directly corroborates the crucial role of MxiH in MxiC release prior to effectors secretion. The *mxiC^{F206S}* mutant is unable to control effectors secretion but can still secrete translocators/effectors in response to CR induction. We subsequently investigated whether or not the introduction of the F206S mutation in the *mxiH^{K69A}* background would restore effectors secretion. The *mxiC mxiH* double mutant construction did not induce proteins secretion and this was restored to wild-type state by pYC163 plasmid producing native MxiC and MxiH (Fig. 4A). Not surprisingly, the *mxiH mxiC* mutant expressing MxiC^{F206S}–MxiH (pYC166) or MxiC–MxiH^{K69A} (pYC165) exhibited the single *mxiC^{F206S}* or *mxiH^{K69A}* phenotype respectively (Fig. 4A). Upon CR induction, the secretion of early effectors was restored in strain *mxiH^{K69A} mxiC^{F206S}* (pSL164) (Fig. 4A). As MxiC^{F206S} does not interact with MxiI, our results suggest that MxiC–MxiI complex dissociation is required for switching to effectors secretion. Unexpectedly, MxiC^{F206S} was not secreted in the *mxiH^{K69A}* background even though it was produced at wild-type level (Fig. 4B). The data presented here suggests that MxiC secretion is not a prerequisite for the switch to effectors secretion.

Exclusive translocators secretion in the mxiI^{Q67A} background

The effect of the needle mutants (*mxiH^{K69A}, mxiH^{R83A}, mxiH^{P44A}, mxiH^{Q51A}*) in the regulation of secretion was previously reported (Kenjale *et al*., 2005). As MxiH and MxiI share around 20% sequence identity (Fig. 5A), we investigated whether or not selective mutations of MxiH's conserved residues within MxiI might also affect secretion. While residues K69 and R83 are not conserved in MxiI, P44 and Q51 correspond to MxiI residues P60 and Q67 respectively. To test this hypothesis, we first constructed a low-copy plasmid, pSM6, expressing MxiI that restores the secretion defect of the *mxiI* mutant (Fig. 5B). To avoid the potential effect of P60 mutation on the structure of MxiI, we replaced residue Q67 by an Alanine (pSM33) and further tested the strain *mxiI^{Q67A}* for its secretion ability. Proteins analysis of the *mxiI^{Q67A}* strain revealed that in response to CR induction, secretion of IpaA was reduced, and IcsB, MxiC and OspD1 were dramatically affected, while IpaB secretion remained unaffected (Fig. 5B). The observed reduction in secretion was not associated with the lack of proteins production as shown in Fig. 5C. As a control, we monitored the presence of the cytoplasmic marker DnaK protein in both cells lysate and supernatant fractions. Our results clearly show the absence of any cytoplasmic material in the supernatant fractions (Fig. 5B). We conclude that although secretion of IpaA appeared slightly different (Figs 4B and 5B), the *mxiH^{K69A}* and *mxiI^{Q67A}* mutants exhibit almost a similar phenotype.

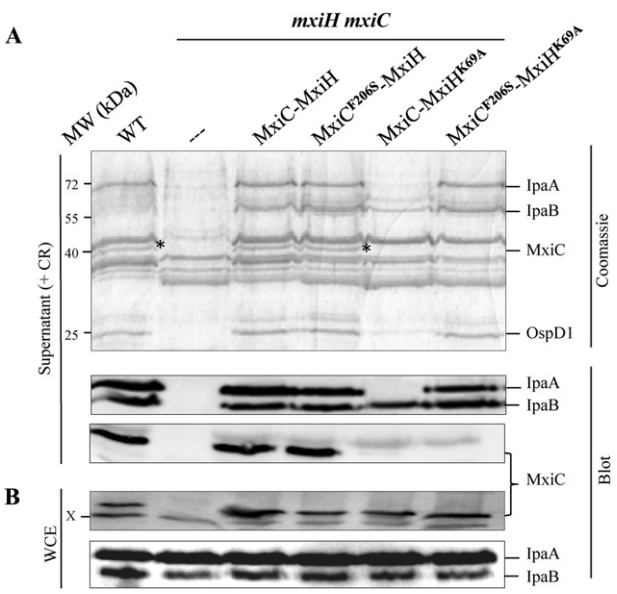

Fig. 4. Mutation *mxiC^{F206S}* restores effectors secretion in the *mxiH^{K69A}* background. (A) Congo red induced supernatants (+ CR) or (B) bacterial whole-cell extracts (WCE) of strains: wild-type (WT), *mxiC mxiH* double mutant, and its derivatives complemented with plasmid expressing native MxiC and MxiH (pYC163) or its derivatives expressing MxiC^{F206S} and MxiH (pYC166), MxiC and MxiH^{K69A} (pYC166) or MxiC^{F206S} and MxiH^{K69A} (pSL164), were resolved on SDS-PAGE and analysed by Coomassie blue staining or by Western blot using polyclonal antibodies directed against IpaA, IpaB and MxiC. X indicates the position of a non-specific band recognized by the anti-MxiC polyclonal antibodies. The asterisk (*) indicates the position of MxiC or MxiC^{F206S}. All experiments were performed at least three times.

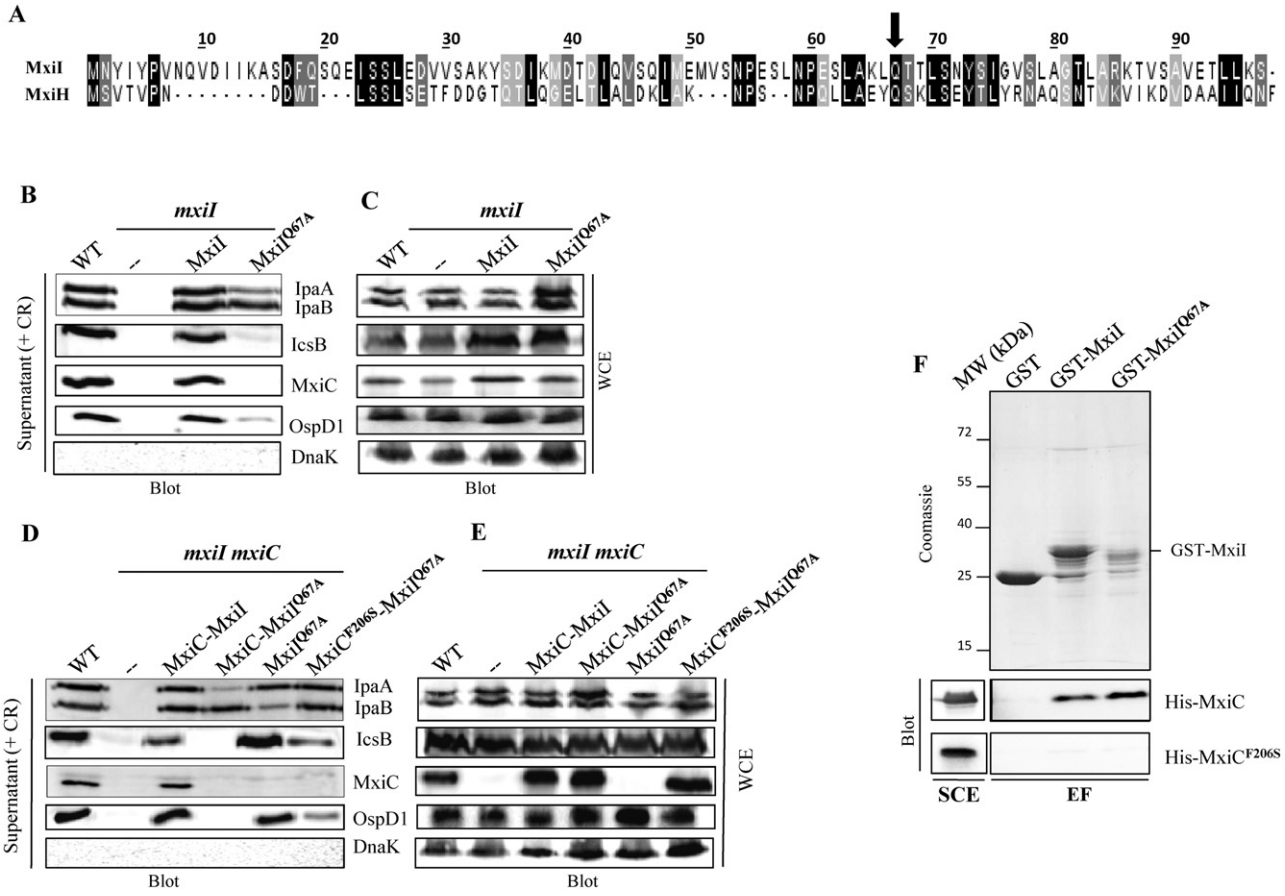

Fig. 5. Mutation *mxiC*^{F206S} restores effectors secretion in the *mxiI*^{Q67A} background.
A. Sequence alignment of MxiH and MxiI using CLUSTALW2 and Jalview programs. Residues are boxed in black (identity) and grey scale (similarity score). Arrow points to residue Q67 of MxiI (Q51 in MxiH) mutated in this study. Proteins of the CR supernatants and whole-cell extracts (WCE) were analysed by Western blot using antibodies directed against IpaB, IpaA, IcsB, MxiC and OspD1. The anti-DnaK antibody was used here as a cytoplamic marker.
B–E. Strains used are: (B and C) wild-type (WT), the *mxiI* mutant, *mxiI*/pSM6 (MxiI) and *mxiI*/pSM33 (MxiI^{Q67A}), (D and E) the *mxiC mxiI* double mutant and its derivatives harbouring plasmids pF13b and pSM6 expressing MxiC and MxiI respectively; or their variants expressing MxiC and MxiI^{Q67A}, MxiI^{Q67A} or MxiC^{F206S} and MxiI^{Q67A}.
F. SCEs of *E. coli* producing His-MxiC or His-MxiC^{F206S} were incubated with GST-MxiI, GST-MxiI^{Q67A} or GST alone bound to gluthatione-Sepharose. Eluted fractions (EF) were analysed as described in Fig. 3.
Proteins analysis and GST pull-down experiments were performed at least three times.

Mutation mxiC^{F206S} *restores effectors secretion in the mxiI*^{Q67A} *background*

To further investigate the phenotype of the *mxiI*^{Q67A} mutant, we constructed an *mxiI mxiC* double mutant (see *Experimental procedures*) that did not secrete proteins. This phenotype was restored to wild-type state by expression of native MxiI and MxiC from plasmids pSM6 and pF13b respectively (Fig. 5D). As expected, in the absence of MxiC, *mxiI mxiC*/pSM33 (MxiI^{Q67A}) secreted IpaB, IpaA, IcsB and OspD1 (Fig. 5D). Comparatively, wild-type secretion of IpaB and IpaA and a reduced secretion of IcsB and OspD1 were observed in the *mxiC*^{F206S} *mxiI*^{Q67A} background (Fig. 5D). Interestingly, MxiC^{F206S} was not secreted in the *mxiI*^{Q67A} background, although it was produced at wild-type level (Fig. 5D and E). Lastly, using GST pull-down assay, we found that MxiI^{Q67A} interacts with His-MxiC, but not with the His-MxiC^{F206S} variant (Fig. 5F).

The interaction between MxiI and MxiC homologues occurs in Salmonella *and* Yersinia

As mutants in *invE* of *Salmonella* and in *yopN* of *Yersinia* exhibit a deregulated secretion phenotype (Forsberg *et al.*, 1991; Kubori and Galan, 2002), we investigated whether, as for MxiC, InvE and YopN may also interact with MxiI counterparts PrgJ and YscI respectively. Hence, we constructed four plasmids producing GST-PrgJ, His-InvE, GST-YopN and His-YscI. After immobilization on

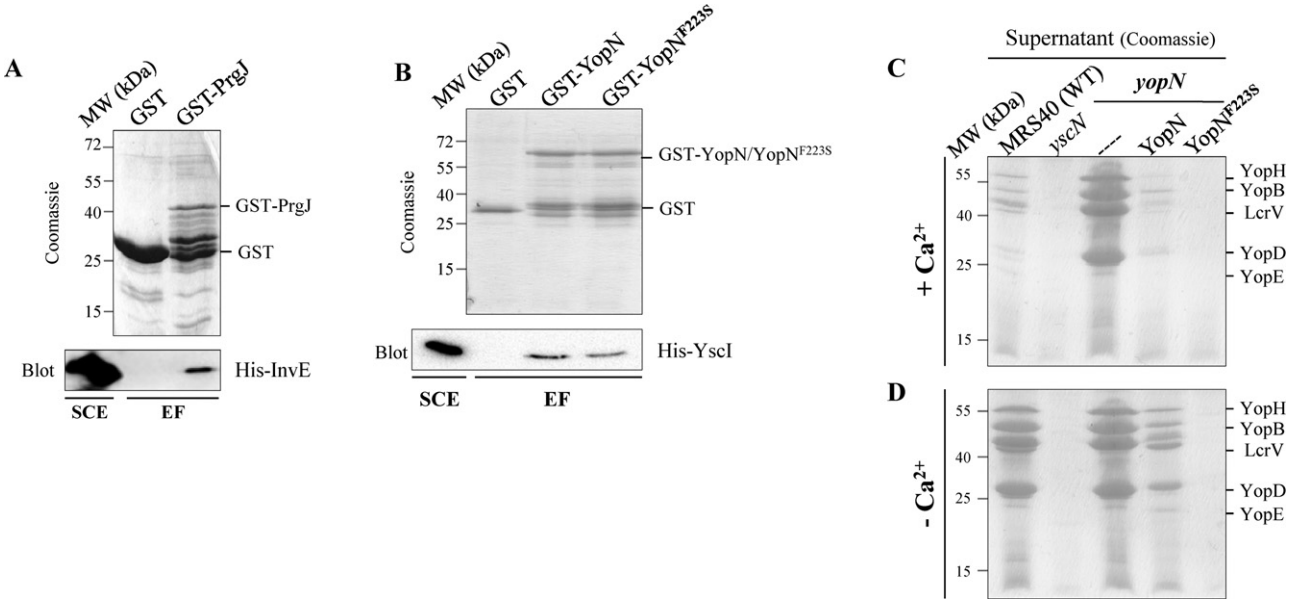

Fig. 6. MxiC homologue proteins in *Yersinia* and *Salmonella* interact with their MxiI counterparts and mutation *yopN*^{F223S} blocks Yop secretion.
A. SCE of *E. coli* producing His-InvE was incubated with GST-PrgJ bound to gluthatione-Sepharose.
B. SCE of *E. coli* producing His-YscI was incubated with GST-YopN or GST-YopN^{F223S} produced in the *Yersinia* background. Eluted fractions (EF) were analysed as previously described in Fig. 3.
C and D. Coomassie blue staining analysis of the supernatant precipitated from *Yersinia enterocolitica* culture grown (C) in the presence of calcium (+ Ca^{2+}) (absence of induction) or (D) in its absence (– Ca^{2+}) (inducible secretion condition). Strains used are wild-type *Y. enterocolitica* (MRS40), the T3S-deficient mutant *yscN*, the *yopN* mutant and its derivatives complemented with plasmid pYC171 (YopN) or pYC174 (YopN^{F223S}).
Shown data were confirmed in three independent experiments.

gluthatione-Sepharose beads, GST-PrgJ was incubated with *E. coli* lysate expressing His-InvE. We found that InvE interacts with GST-PrgJ but not with GST alone (Fig. 6A). As YopN requires specific chaperones for its stability, GST-YopN was produced in the *Y. enterocolitica* background before incubation with His-YscI. We also showed that YscI interacts, either directly or indirectly, with YopN but not with GST alone (Fig. 6B).

Since residue F206 seems crucial for the MxiC–MxiI interaction, we mutated the corresponding residues, Y211 and F223, in His-InvE and in GST-YopN respectively (Fig. 1A). The insolubility of His-InvE^{Y211S} meant that we could not assess its interaction with PrgJ (data not shown). In contrast, we found that GST-YopN^{F223S} interacts with YscI (Fig. 6B). Hence, we postulate here, unlike the *yopN* mutant, *yopN*^{F223S} strain has to control Yop secretion in the absence of induction by calcium (+ Ca^{2+}). To test such hypothesis, we constructed low-copy plasmid pYC171 (YopN) that fully restored the secretion defect of the *yopN* mutant (Fig. 6C). Next, we constructed plasmid pYC174 expressing YopN^{F223S} and showed that Yop secretion was blocked in the *yopN*^{F223S} strain under inducible secretion condition (– Ca^{2+}) (Fig. 6D). As a control, no secretion was observed with the *yscN* T3S deficient secretion mutant.

Secretion of IpaB and IpaC translocators is delayed in the mxiC mutant

In contrast to wild-type *Shigella,* the *mxiC* mutant is not responsive to CR induction and is defective in IpaC secretion. Moreover, it constitutively secretes low levels of IpgD between 2 and 10 min post CR induction (Martinez-Argudo and Blocker, 2010). As MxiC is required in T3S signal transmission, we asked whether this defect could be due to a delay in CR responsiveness. Bahrani *et al.* (1997) previously established that maximal recovery of IpaC in the supernatant fraction is obtained after 30 min of CR induction. Therefore, we lengthened the induction time from 5 to 30 min and analysed the proteins of the supernatant. Our results showed that IpaB, IpaC and IpaD secretion, by the *mxiC* mutant, reached wild-type level within 30 min post induction (Fig. 7). The secretion defect of IpaB, IpaC and IpaD at 5 and 10 min post induction is not due to their expression since they were produced at wild-type level (Fig. 7). Compared to IpaB, IpaC and IpaD, MxiC secretion was delayed in the wild-type strain as it started 10 min post induction (Fig. 7). These results suggest that MxiC is involved in the induction of translocators secretion which appears to be delayed rather than impaired in the *mxiC* mutant. As a

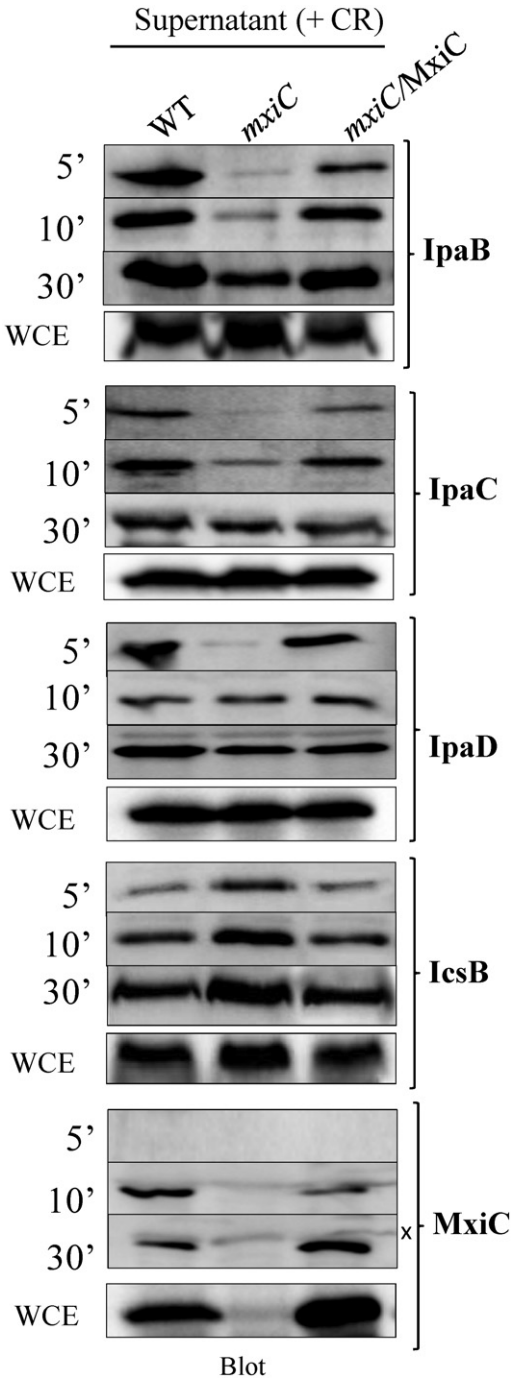

Fig. 7. Secretion of translocators IpaB and IpaC is delayed in the *mxiC* mutant. Bacteria: wild-type strain (WT), the *mxiC* mutant and its derivative complemented with pAB108′ (MxiC) were cultured until an OD_{600} ~ 0.8, centrifuged and the pellets were resuspended in PBS and further incubated during 5, 10 or 30 min with CR to induce proteins secretion. Whole-cell extracts (WCE) and proteins of the supernatants were resolved by SDS-PAGE and analysed by Western blot using polyclonal antibodies directed against IpaB, IpaC, IpaD, MxiC or IcsB. X corresponds to a non-specific band recognized by the anti-MxiC polyclonal antibodies. These experiments were repeated three times.

control, under similar conditions, secretion of the IcsB effector was almost comparable although a slight increase was detected in the *mxiC* mutant background (Fig. 7).

IpgC enhances MxiC interaction with ATPase Spa47 and regulates translocators secretion

To investigate the mechanism by which MxiC regulates IpaB and IpaC secretion, we took advantage of the direct interaction that we previously reported (Botteaux *et al*., 2009) between the ATPase Spa47 and MxiC. The significance of this interaction remained only speculative and needs to be further clarified. As this interaction is hardly seen in *E. coli*, we assessed it in the *Shigella* background. We found that the interaction is enhanced suggesting the existence of an additional specific *Shigella* component that stabilizes the complex (Fig. 8A). Taking into account that MxiC regulates the secretion of IpaB and IpaC, we next assessed Spa47–MxiC interaction in *E. coli* strain harbouring the pHI1 plasmid encoding the translocator chaperone (His-IpgC). We incubated GST alone or GST-Spa47 with His-IpgC and MxiC-FLAG either independently, simultaneously or sequentially, before analysing the eluted fractions using anti-His and anti-FLAG antibodies (Fig. 8B and C). Hereby, we demonstrated that MxiC efficiently interacts with Spa47 in the *Shigella* background when Spa47 is already complexed to IpgC (Fig. 8B and C, lane 4). In contrast, the interaction of Spa47 with the preformed MxiC–IpgC complex was undetectable (Fig. 8B and C, lane 3). It is worth noting that the interaction between Spa47 and IpgC is reported here for the first time.

Lastly, to investigate whether MxiC interacts directly with IpgC, we performed a GST pull-down assay which revealed a direct interaction between His-MxiC and GST-IpgC (Fig. 8D). In parallel, we also found that His-$MxiC^{F206S}$ interaction with GST-IpgC remained unaffected (Fig. 8D).

Discussion

We have previously reported that *mxiC* gene deletion deregulates secretion of early and late effectors in the absence of T3S induction highlighting the crucial role of MxiC in the control of effectors release (Botteaux *et al*., 2009). However, the molecular mechanism remained uncharacterized. Here, we report for the first time an interaction between the predicted inner-rod component MxiI and the gatekeeper MxiC. We also demonstrated that such interaction is potentially involved in the secretion switch from translocators to effectors. Mutational analysis also reveals that the inability to control effectors secretion by the $MxiC^{F206S}$ variant whose folding was not affected compared with native MxiC, is likely due to its lack of

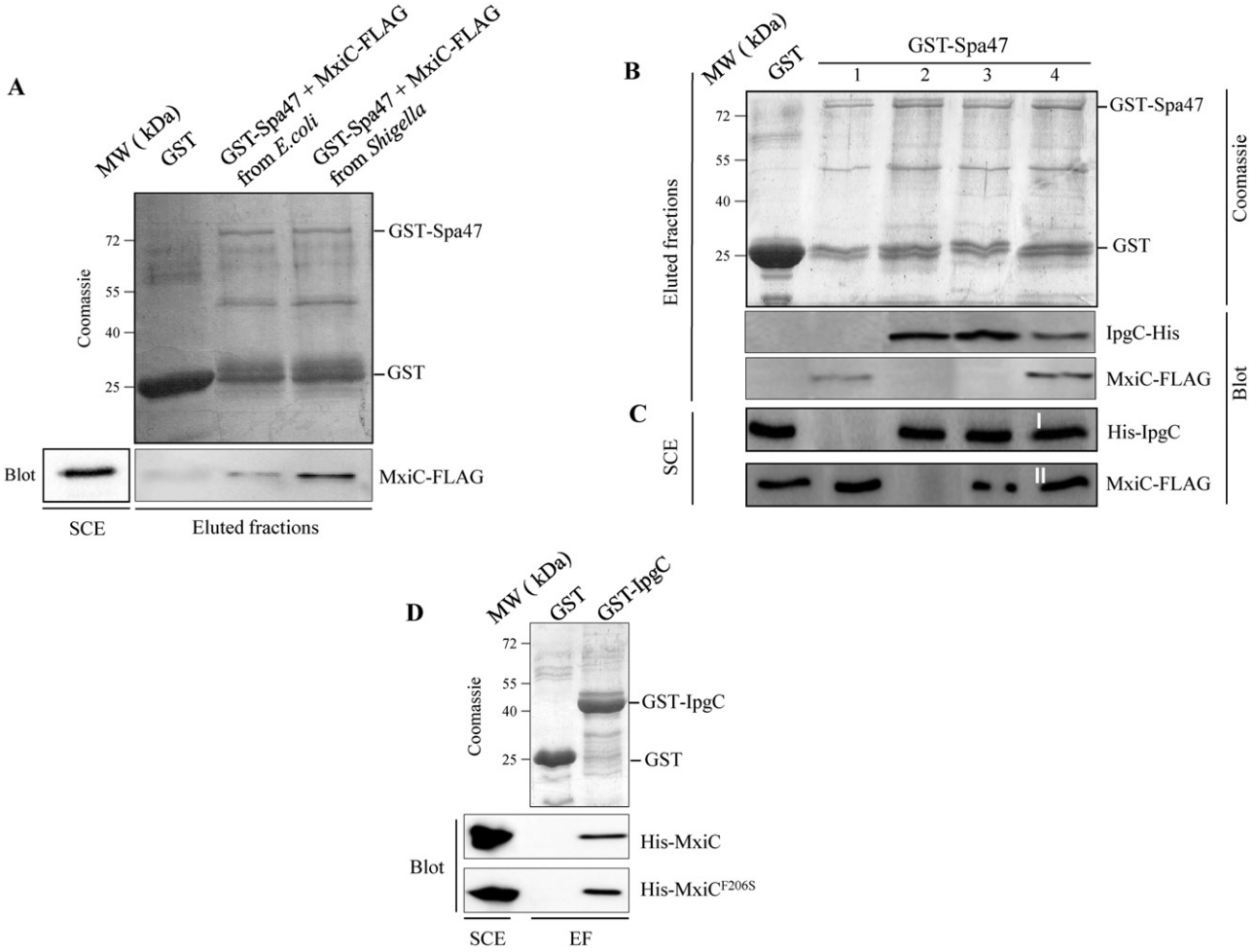

Fig. 8. The interaction between MxiC and Spa47 is enhanced in the presence of chaperone IpgC.
A. Soluble cell extracts (SCEs) of *E. coli*, or the *mxiC* mutant producing MxiC-FLAG from the pYC130 plasmid were incubated with either GST-Spa47 or GST alone bound to gluthatione-Sepharose.
B and C. SCEs of *E. coli* expressing His-IpgC and MxiC-FLAG were incubated with GST-Spa47 bound to gluthatione-Sepharose. either individually (lanes 1 and 2) or simultaneously (lanes 3 and 4). Lane 3: GST-Spa47 was incubated with a mixture of SCEs containing both His-IpgC and MxiC-FLAG (C). Lane 4: SCE containing His-IpgC was pre-incubated with bound GST-Spa47 (I) and mixed, in a second step (II), with SCE containing MxiC-FLAG. Eluted fractions (EF) were analysed by Western blot using anti-FLAG and anti-His antibodies.
D. SCEs of *E. coli* producing His-MxiC and His-MxiC^{F206S} were incubated with GST-IpgC or GST alone bound to gluthatione-Sepharose. Eluted fractions (EF) were analysed by Western blot using an anti-His monoclonal antibody.
These results were confirmed in several independent experiments.

interaction with MxiI. This suggests that in the absence of T3S induction, MxiI–MxiC complex is docked at the T3SA entry gate forming a plug that would specifically prevent effectors secretion. Upon T3S induction, MxiC is probably detached from MxiI which consequently opens the gate for effectors release. For timely secretion, MxiC is likely to receive a signal from the tip complex. Interestingly, several studies have suggested that the needle itself is required for signal transmission from T3SA tip to base but the underlying mechanism remains unknown (Martinez-Argudo and Blocker, 2010). Even though MxiI has never been precisely localized at the *Shigella* T3SA base, its counterpart PrgJ in *Salmonella* was shown to be part of the inner-rod and to stabilize the needle structure (Marlovits *et al.*, 2004). In the *Salmonella* needle structure study, it was suggested that the large plasticity in how subunits are locally packed around the canal could be responsible for signal transmission along the needle (Kimbrough and Miller, 2002). Obviously, such a signal must go down from the tip to base through MxiH and MxiI. In support of this hypothesis, two mutations within *mxiH* (K69A and R83A) prevent early effectors secretion (Kenjale *et al.*, 2005). Such a mechanism is likely achieved by sequestering MxiC within the bacterial cytoplasm. Indeed, Martinez-Argudo and Blocker (2010) reported that this defect can be reverted by deleting the *mxiC* gene in the *mxiH*^{K69A} and

mxiH^{R83A} backgrounds. Here, we demonstrate that effectors secretion can be recovered in the *mxiH*^{K69A} *mxiC*^{F206S} background, which can be explained at least by the inability of MxiC^{F206S} to interact with MxiI. Besides, K69A mutation may cause potential loss of plasticity between the needle and inner-rod subunits which blocks the activation signal transmission and subsequently affects the dissociation of MxiC–MxiI complex. Alternatively, we cannot exclude that MxiH^{K69A} no longer receives the activation signal from the tip complex.

In the course of this study, we generated the *mxiI*^{Q67A} strain that exhibits a closely related phenotype to the *mxiH*^{K69A} effector mutant. This is the first report demonstrating that a single mutation within the inner-rod component deregulated secretion. Effectors secretion was also recovered in the *mxiI*^{Q67A} background either by deleting the *mxiC* gene or upon coexpressing MxiC^{F206S} variant. Comparatively, the mutation *yscI*^{Q84A} in *Yersinia* corresponding to *mxiI*^{Q67A} only reduces Yop secretion (Wood *et al*., 2008).

As mutants in genes encoding *mxiC* homologues in other pathogens also deregulate effectors secretion, we investigated whether or not equivalent MxiC–MxiI interaction may also take place in *Yersinia* and *Salmonella*. We demonstrate here that MxiC–MxiI interaction occurs in both bacteria suggesting the existence of a shared mechanism regulating the switch to effectors secretion. In *Yersinia,* numerous mutations within highly conserved residues of YopN block Yop secretion by a mechanism that remains poorly understood (Ferracci *et al*., 2005). Accordingly, we have shown here that YopN^{F223S} mutation also blocks Yop secretion. In contrast to MxiC^{F206S}, YopN^{F223S} still interacts with YscI, suggesting that YscI-YopN^{F223S} may form a complex that sticks at the T3SA entry gate to block Yop secretion. It is also worth noting that, due to proteins complex instability in *E. coli,* the interaction assay was performed using GST-YopN or GST-YopN^{F223S} produced in the *Yersinia* background. Thus, the interaction observed between YscI and YopN^{F223S}, in contrast to *Shigella*, may involve additional T3S partners such as SycN or SycB which are of course missing in *Shigella.* Comparatively, the MxiC^{Y185N} variant, corresponding to the YopN^{Y202N} that also prevents Yop secretion in *Yersinia,* only deregulates effectors secretion in *Shigella.* Therefore, our findings contribute to unravel the mechanism involved in blocking Yop secretion.

To date, InvE (MxiC counterpart) was not detected in *Salmonella* secreted fraction supporting the fact that gatekeeper secretion is not a prerequisite for its function. In the *mxiI* or *mxiH* 'effector mutants', MxiC and MxiC^{F206S} secretion is totally abolished while only MxiC^{F206S} expression restored effectors secretion. Knowing that MxiC^{F206S} lost its ability to interact with MxiI^{Q67A} or MxiI and promotes effectors secretion, the activation signal could be facilitated via MxiC detachment from MxiI rather than MxiC secretion *per se*. Accordingly, while MxiC^{F206S} secretion was significantly reduced compared to MxiC in the wild-type background, effectors were equally secreted upon T3S induction. This could be explained by the inability of MxiC^{F206S} to interact with MxiI, which would consequently limit its own recruitment to the T3SA entry gate. In this case, instead of being secreted MxiC^{F206S}, might be preferentially taken up by the Spa47–IpgC complex.

The *mxiC* mutant is known to secrete translocators in response to CR induction within 10 min (Martinez-Argudo and Blocker, 2010). In the present study, we have demonstrated that secretion of translocators released by the *mxiC* mutant reaches wild-type level at 30 min post CR induction. Both IpaB and IpaC interact with IpgC and the dissociation of these complexes *in vitro* implies various physical events (Birket *et al*., 2007). The latter is poorly understood *in vivo* but is believed to be achieved via the ATPase Spa47 complex. Here, we identify an unexpected role of IpgC in stabilizing Spa47 interaction with MxiC. The absence of a direct interaction between Spa47 and MxiC (Fig. 8, line 3) could be explained by the fact that the conformation adopted by the preformed IpgC–MxiC complex in *E. coli* is not suitable for such a complex. However, MxiC-FLAG, produced in the *Shigella* background, interacts with Spa47 which is likely to be in a complex with IpgC-translocators. Thus, it is tempting to speculate that, under physiological conditions, two events might occur: (i) MxiC interacts with the complex Spa47–IpgC-translocators, and (ii) MxiC displaces translocators to promote their secretion upon T3S induction. Such a mechanism of action is supported by the fact that *mxiC* mutant expressing MxiC^{F206S}, which still interacts with IpgC, remains responsive to CR induction. Comparatively, different links between MxiC and the translocators were previously reported. These include, for example, the interaction between InvE (MxiC) and SicA (IpgC) in *Salmonella* (Kubori and Galan, 2002), the interaction between CopN (MxiC) and Ssc3 (IpgC) in *Chlamydia* (Archuleta *et al*., 2011) and the interaction between the chaperone TyeA (MxiC^{XB3}) and YopD (IpaC) in *Yersinia*. Collectively, these results suggest the existence of a shared mechanism regulating the hierarchy of translocators secretion.

Altogether, our findings contribute to the emerging general pattern related to the T3S hierarchy (Fig. 9). Briefly, before T3S induction, MxiC is engaged in a complex with MxiI at the T3SA entry gate to prevent effectors secretion. A first pool of IpaB and IpaC is already exposed at the tip of the needle to sense CR or host cell contact, while a second one, bound to IpgC, remains stored in the cytoplasm. Upon T3S induction, an activation signal is allosterically transmitted from the tip complex to MxiH, then to MxiI, and finally to MxiC. At this stage, we may consider that MxiC is partly attached to Spa47 which

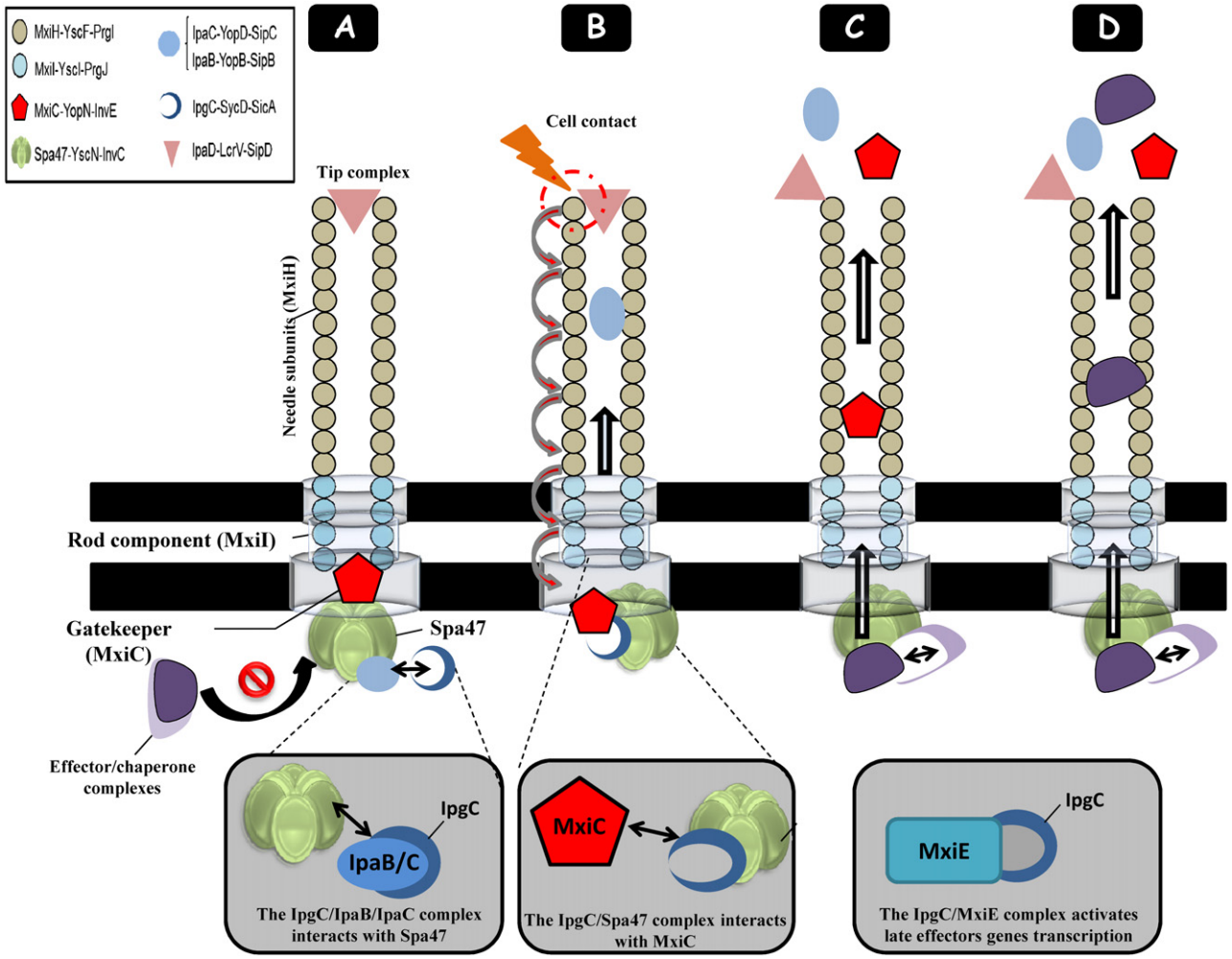

Fig. 9. Proposed general events following transmission of the activation signal from the T3SA needle tip to the base.
A. Double locked T3SA channel by the tip complex at the needle tip and by the gatekeeper at the base.
B. Activation of the T3SA upon host cell contact or CR inducer, the tip complex transmits a signal through the needle to release the gatekeeper (MxiC) from the rod component (MxiI). Free MxiC will bind IpgC to enhance translocators IpaB and IpaC secretion.
C and D. Once MxiC, OspD1 and early effectors are secreted; released IpgC will bind to MxiE to induce transcriptional activation of late effectors genes. Counterparts of eight key conserved *Shigella* components (MxiH, MxiI, MxiC, Spa47, IpaC, IpaB, IpgC and IpaD) are mentioned for *Yersinia enterocolitica* and *Salmonella* respectively.

would facilitate IpaB and/or IpaC detachment from IpgC. Once translocators are secreted, MxiC is released from Spa47 and early effectors secretion follows. In parallel, following the anti-activator OspD1 and MxiC secretion, free IpgC will subsequently bind to the transcriptional activator MxiE to initiate transcription, production and finally secretion of late effectors.

In summary, the present work reports the identification of a novel mechanism involved in effectors sequestration prior to T3S induction. This implies the blockade of the T3SA entry gate upon intimate interaction between the gatekeeper MxiC and MxiI. For the first time, our results depict, a new discrete step, involving MxiC interacting to IpgC to control translocators secretion. Collectively, the present work opens new research avenues for future studies focusing on the real-time localization of MxiC during the major secretion steps. Crystal structure resolution of MxiI (parental versus MxiI^{Q67A}) either alone or in complex with MxiC should aid to understand why the activation signal transmission is blocked in the *mxiI*^{Q67A} mutant. The first switch in secretion from the needle to translocators is known to be controlled by the Spa40–Spa32 complex and these proteins are conserved among several bacterial T3SSs (Kubori *et al.*, 2000; Edqvist *et al.*, 2003; Botteaux *et al.*, 2008; Lorenz and Buttner, 2011). The switch in substrate specificity in *Yersinia* involves YscP (Spa32) and YscU (Spa40) who exert their effects on substrate export by controlling YscI secretion (Wood *et al.*, 2008). Interestingly, HrpB2 (MxiI) of the plant pathogen *Xanthomonas campestris* pv. *vesicatoria* was shown to

interact with the cleaved form of HrcU (Spa40) (Lorenz *et al.*, 2008). More recently, it was suggested that the inner-rod component EscI (MxiI) of EPEC may be involved in substrate secretion switch via its interaction with EscU (Spa40) (Sal-Man *et al.*, 2012). Under our hands, we confirmed the interaction between MxiI and the cleaved forms of Spa40 (data not shown), supporting the broad implication of the rod component in the T3S switches. Thus, it will also be important to address the link between MxiI and the Spa40–Spa32 complex in relation to the first secretion switch from needle to translocators. Answering these queries will certainly improve our knowledge and understanding of the secretion hierarchy mechanisms.

Experimental procedures

Strains and bacterial growth conditions

The list of *E. coli*, *Shigella flexneri* and *Y. enterocolitica* strains used in this study is shown in Table S1. *Shigella* strains were phenotypically selected on Congo red agar plates (Meitert *et al.*, 1991) and grown in Trypticase Soy Broth (VWR) with the antibiotics at the following concentrations: ampicillin, 100 μg ml^{-1}; kanamycin, 50 μg ml^{-1}; streptomycin, 100 μg ml^{-1}; zeocin, 50 μg ml^{-1}, chloramphenicol, 25 μg ml^{-1} for *E. coli* strains and 3 μg ml^{-1} for *Shigella* strains. *Yersinia* strains were grown routinely in BHI (Brain Heart Infusion) Broth or TSA plates at a temperature of 26°C or 37°C respectively.

Construction of the mxiC mxiH and mxiC mxiI double mutants

The suicide vector pMS017 (pGP704-*mxiC*::*ble*) (Botteaux *et al.*, 2009) was transferred to the *mxiH::aphA3* or *mxiI::aphA3* mutant (Blocker *et al.*, 2001) by conjugal mating. Transconjugants were first selected for their resistance to zeocin and streptomycin. Clones in which a double recombination event had exchanged the wild-type *mxiC* gene by the mutated copy of the pMS017 were identified by screening for sensitivity to ampicillin. The structure of pWR100 derivatives carrying the double *mxiH mxiC* or *mxiI mxiC* mutation was confirmed by PCR.

Plasmids construction

The plasmids and primers used in this study are listed in Tables S1 and S2. Plasmid pAB108′ (pSU18-*mxiC*), used to complement the *mxiC* mutant, was constructed by inserting a digested PCR fragment, carrying native *mxiC* gene, into the EcoRI/SalI sites of the low-copy vector pSU18 (Invitrogen). Plasmid pYC163, encoding both native MxiC and MxiH, was used to complement the *mxiC mxiH* mutant. This was constructed in two steps. First, plasmid (pSU18-*mxiC*) was constructed by inserting the *mxiC* gene obtained by PCR into EcoRI/KpnI digested pSU18. Then, the latter was used to insert a PCR-amplified *mxiH* gene into the KpnI/SalI sites of pSU18-*mxiC*. Plasmid pSM6, encoding native MxiI, was used to complement the *mxiI* mutant. The latter was obtained by cloning *mxiI* PCR digested DNA fragment into the pSU18 vector.

Recombinant (GST, His or FLAG) proteins, used in the interaction assays, were produced from plasmids listed in Table S1. Plasmids expressing GST fused to MxiI, MxiH, MxiC, IpgC, Spa47, YopN, YopN^{F223S} or PrgJ were constructed by inserting PCR digested DNA fragments into the pGEX4T1 expressing vector. Plasmids expressing His6 fused to MxiC, MxiI, MxiH, InvE and YscI were constructed by inserting PCR digested DNA fragments into the pET30 vector expressing His6 recombinant proteins. Plasmid pYC130 expressing MxiC-FLAG was constructed by inserting a PCR digested DNA fragment into the pUC18K2 plasmid (Menard *et al.*, 1993).

Directed mutagenesis was carried out according to the procedure of the Quick Change Mutagenesis kit (Stratagene). The use of each primer in PCR creates a restriction site (see Table S2) to easily confirm the introduced mutation. Single directed mutagenesis of residues F206S (MxiC) and/or K69A (MxiH) were carried out on plasmids pAB108′ (pSU18-*mxiC*), pYC163 (pSU18-*mxiC-mxiH*), pSL30 (pET30-MxiC) and pF13b (pUC19-MxiC) (Botteaux *et al.*, 2009). The resulting plasmids were named pAB130 (pSU18-MxiC^{F206S}), pYC166 (pSU18-MxiC^{F206S}-MxiH), pYC165 (pSU18-MxiC-MxiH^{K69A}), pSL164 (pSU18-MxiC^{F206S}-MxiH^{K69A}), pAB133 (pET30-MxiC^{F206S}) and pAB93 (pUC19-MxiC^{F206S}). Mutations Y185N, M226A, G239A and L245A within MxiC were carried out on pAB108′ (pSU18-*mxiC*). Mutation Q67A of *mxiI* was carried out on pSM6 and the resulting plasmid was named pSM33. Plasmid pYC171 encoding native YopN was constructed by inserting a PCR digested DNA fragment encompassing the *yopN* gene of *Y. enterocolitica* into the pSU18 EcoRI/SalI digested vector. The latter was used to generate, by directed mutagenesis, plasmid pYC174 encoding YopN^{F223S}.

Protein analysis

Crude extracts and culture supernatants of *S. flexneri* strains were prepared and analysed as previously described (Allaoui *et al.*, 1992). For the induction with Congo red (CR), bacteria were grown until OD_{600} has reached 2 units, harvested by centrifugation, resuspended in PBS containing 200 μg ml^{-1} CR, and incubated for 10–30 min at 37°C. Bacteria were centrifuged at 13 000 *g* for 15 min at 4°C and proteins present in the supernatant were analysed by SDS-PAGE. Western blotting was performed on PVDF membranes (Roche) and developed using chemiluminescence (Perkin Elmer). Immunodetection were carried out as described by Botteaux *et al.* (2009) using monoclonal antibodies (mAbs) directed against IpaB and His6 motif and a serial of polyclonal antibodies against IpaC, IpaD, IpaA, MxiC, IpaH9.8, OspD1, DnaK, IcsB, GST or the FLAG motif.

Protein production and GST pull-down assays

Escherichia coli BL21 (DE3 Rosetta) were transformed with pGEX4T1 plasmid encoding GST alone or its derivatives encoding GST fusion proteins and grown in 100 ml of LB to OD_{600} ~ 0.7 at 37°C. Protein expression was induced with 0.1 mM isopropyl β-D-1-thiogalactopyranoside (IPTG) for 3 h at 37°C. Cells were harvested, resuspended in lysis buffer (40 mM Tris pH 8.0, 500 mM NaCl, 1 mM EDTA) and then lysed by sonication. A final concentration of 1% Triton X-100

was added to the lysate followed by incubation on ice for 20 min. The lysates were then clarified by centrifugation and the supernatants mixed with gluthatione sepharose 4B matrix beads (GE Healthcare) previously equilibrated with PBS buffer. The mixtures were incubated overnight at 4°C in a rotor-shaker with bacterial lysates producing His- or FLAG-tagged recombinant proteins. Beads were washed eight times and proteins eluted by incubating beads 10 min with elution buffer (40 mM Tris pH 8.0, 500 mM NaCl and 50 mM reduced glutathione). The eluted proteins were resolved by SDS-PAGE and analysed by Coomassie blue staining or Western blotting.

Protein folding analysis by fluorescence spectroscopy

Bacteria harbouring plasmids pSL30 and pAB133, expressing His-MxiC and His-MxiC^{F206S} proteins, respectively, were grown overnight at 37°C with shaking (200 r.p.m.). The subculture was then used to inoculate 1 l of LB culture and subsequently grown until the optical density (OD_{600}) of 0.6 was reached. Proteins expression was induced by adding 1 mM IPTG at 37°C during 3 h. Cells were subsequently harvested by centrifugation for 10 min at 8500 r.p.m and the pellets were resuspended in 50 mM Tris-HCl buffer at pH 8.0, containing 500 mM NaCl, 20 mM imidazole and proteases inhibitors cocktail. After lysis by sonication, the unbroken cells were removed with a low speed centrifugation at 8500 r.p.m. for 60 min. The protein mixture was applied to FPLC chromatography on a HisTrap column (5 ml; GE Healthcare) equilibrated with 50 mM Tris-HCl buffer at pH 8.0, containing 500 mM NaCl, 20 mM imidazole. His-MxiC and His-MxiC^{F206S} were eluted with a linear gradient of 0.02–500 mM imidazole in 50 mM Tris-HCl buffer at pH 8.0, containing 500 mM NaCl. The eluted proteins fractions, as revealed by SDS-PAGE, were pooled and subsequently concentrated by ultrafiltration using Centricon® centrifugal concentrator (30 kDa molecular mass cut-off) against 50 mM Tris-HCl buffer at pH 8.0, containing 500 mM NaCl and loaded on a FPLC Superdex200 column (120 ml; GE Healthcare) equilibrated with 50 mM Tris-HCl buffer at pH 8.0, containing 500 mM NaCl. The eluted fractions containing His-MxiC or His-MxiC^{F206S} were pooled and concentrated by ultrafiltration against PBS buffer at pH 7.4 (Fig. 2A). Protein concentration was determined spectrophotometrically using a molar extinction coefficient at 280 nm of 20 400 M^{-1} cm^{-1} (Gill and von Hippel, 1989) for purified proteins. A final yield of 3 mg per litre of each purified protein was obtained.

To investigate His-MxiC and His-MxiC^{F206S} folding, the corresponding purified proteins were analysed by fluorescence spectroscopy at a constant temperature of 25.0 ± 0.1°C using a Shimadzu spectrofluorimeter, model RF-5001PC. The fluorescence spectra were obtained with 1 µM final protein concentration. For tryptophan fluorescence measurements, protein solutions were prepared in PBS buffer at pH 7.4. Spectra were recorded between 270 and 500 nm using an excitation wavelength of 285 nm. The excitation and the emission slit widths were 5 nm. The second approach used to assess possible protein misfolding was based on the anilino-8-naphthalenesulphonic acid (ANS, from Sigma-Aldrich, Steinhein, Germany) binding experiments (Azarkan *et al*., 2006). In aqueous solution and/or in the presence of native or completely unfolded proteins, the hydrophobic dye ANS is characterized by a low quantum yield and an emission λmax at about 520 nm. Partitioning of this probe into the hydrophobic core of a protein, e.g. when it forms a molten globule state, enhances its fluorescence intensity and induces a blue shifting of its maximum wavelength, typically from 520 nm to 470 nm. The molar ratio of protein and ANS used was 1:50. ANS concentration was determined spectrophotometrically using a molar extinction coefficient at 350 nm of 5000 M^{-1} cm^{-1}. The excitation was set at 370 nm and the emission spectra were measured in the range 400–600 nm using an excitation and an emission slit widths of 5.0 nm. Both, for tryptophan and ANS binding experiments, a solution without protein was used as a blank and the resulting spectrum was used for fluorescence intensity correction. All used solutions were filtered through 0.2 µm.

Yop *proteins secretion by* Y. enterocolitica

The *Yersinia* supernatants were prepared as previously described (Heesemann *et al*., 1986). Briefly, *Yersinia* was first grown overnight in BHI broth at 26°C with shaking (120 r.p.m.). Next, bacteria were diluted 1:20 in a fresh BHI broth and incubated during 90 min with shaking (120 r.p.m.) at 37°C. After that, the medium was supplemented with EGTA (10 mM) and incubation at 37°C was continued for an additional 90 min. The bacterial cells were then removed by centrifugation (7000 *g*, at 4°C for 20 min). Proteins from the filtrated culture supernatant were precipitated overnight by addition of ammonium sulphate (40% w/v). After centrifugation (10 000 *g* at 4°C for 45 min), the resulting pellets were washed and then resuspended in 50 µl of water respectively. Finally, 15 µl of each fraction was resolved by SDS-PAGE and stained with Coomassie blue.

Acknowledgements

The present work was supported by grants from the 'Fonds National de la Recherche Scientifique – Fonds national Belge de la Recherche Scientifique' (FRS-FNRS; Convention F.3.4556.11) and from the European Community's Seventh framework programme FP7/2011-2015 under grant agreement No. 261742. Y.C., L.S. and S.M., are/were recipients of a PhD fellowship from the Belgian Fonds National de Recherches Industrielles et Agronomiques (FRIA). L.S. received also a funding from the European Community's Seventh framework programme FP7/2011-2015. A.B., L.B. and A.M. are/were Postodoctoral researchers of the FRS-FNRS. A part of this work was also supported by the Fonds Defay and by the Alice and David Van Buuren foundation. Lastly, we are very grateful to Pr. Guy Cornelis for the gift of the *Yersinia* strains and to Drs H. Rahmoune, P. Guest and N. El Hajjami for critical reading of the manuscript.

References

Akeda, Y., and Galan, J.E. (2005) Chaperone release and unfolding of substrates in type III secretion. *Nature* **437:** 911–915.

Allaoui, A., Mounier, J., Prevost, M.C., Sansonetti, P.J., and

Parsot, C. (1992) *icsB*: a *Shigella flexneri* virulence gene necessary for the lysis of protrusions during intercellular spread. *Mol Microbiol* **6:** 1605–1616.
Archuleta, T.L., Du, Y., English, C.A., Lory, S., Lesser, C., Ohi, M.D., *et al.* (2011) The *Chlamydia* effector chlamydial outer protein N (CopN) sequesters tubulin and prevents microtubule assembly. *J Biol Chem* **286:** 33992–33998.
Azarkan, M., Dibiani, R., Goormaghtigh, E., Raussens, V., and Baeyens-Volant, D. (2006) The papaya Kunitz-type trypsin inhibitor is a highly stable beta-sheet glycoprotein. *Biochim Biophys Acta* **1764:** 1063–1072.
Bahrani, F.K., Sansonetti, P.J., and Parsot, C. (1997) Secretion of Ipa proteins by *Shigella flexneri*: inducer molecules and kinetics of activation. *Infect Immun* **65:** 4005–4010.
Birket, S.E., Harrington, A.T., Espina, M., Smith, N.D., Terry, C.M., Darboe, N., *et al.* (2007) Preparation and characterization of translocator/chaperone complexes and their component proteins from *Shigella flexneri*. *Biochemistry* **46:** 8128–8137.
Blocker, A., Jouihri, N., Larquet, E., Gounon, P., Ebel, F., Parsot, C., *et al.* (2001) Structure and composition of the *Shigella flexneri* 'needle complex', a part of its type III secreton. *Mol Microbiol* **39:** 652–663.
Blocker, A.J., Deane, J.E., Veenendaal, A.K., Roversi, P., Hodgkinson, J.L., Johnson, S., and Lea, S.M. (2008) What's the point of the type III secretion system needle? *Proc Natl Acad Sci USA* **105:** 6507–6513.
Botteaux, A., Sani, M., Kayath, C.A., Boekema, E.J., and Allaoui, A. (2008) Spa32 interaction with the inner-membrane Spa40 component of the type III secretion system of *Shigella flexneri* is required for the control of the needle length by a molecular tape measure mechanism. *Mol Microbiol* **70:** 1515–1528.
Botteaux, A., Sory, M.P., Biskri, L., Parsot, C., and Allaoui, A. (2009) MxiC is secreted by and controls the substrate specificity of the *Shigella flexneri* type III secretion apparatus. *Mol Microbiol* **71:** 449–460.
Buchrieser, C., Glaser, P., Rusniok, C., Nedjari, H., D'Hauteville, H., Kunst, F., *et al.* (2000) The virulence plasmid pWR100 and the repertoire of proteins secreted by the type III secretion apparatus of *Shigella flexneri*. *Mol Microbiol* **38:** 760–771.
Buttner, D. (2012) Protein export according to schedule: architecture, assembly, and regulation of type III secretion systems from plant- and animal-pathogenic bacteria. *Microbiol Mol Biol Rev* **76:** 262–310.
Cheng, L.W., Kay, O., and Schneewind, O. (2001) Regulated secretion of YopN by the type III machinery of *Yersinia enterocolitica*. *J Bacteriol* **183:** 5293–5301.
Cornelis, G.R. (2006) The type III secretion injectisome. *Nat Rev Microbiol* **4:** 811–825.
Day, J.B., and Plano, G.V. (1998) A complex composed of SycN and YscB functions as a specific chaperone for YopN in *Yersinia pestis*. *Mol Microbiol* **30:** 777–788.
Deane, J.E., Roversi, P., King, C., Johnson, S., and Lea, S.M. (2008) Structures of the *Shigella flexneri* type 3 secretion system protein MxiC reveal conformational variability amongst homologues. *J Mol Biol* **377:** 985–992.
Deane, J.E., Abrusci, P., Johnson, S., and Lea, S.M. (2010) Timing is everything: the regulation of type III secretion. *Cell Mol Life Sci* **67:** 1065–1075.
Demers, B., Sansonetti, P.J., and Parsot, C. (1998) Induction of type III secretion in *Shigella flexneri* is associated with differential control of transcription of genes encoding secreted proteins. *EMBO J* **17:** 2894–2903.
Edqvist, P.J., Olsson, J., Lavander, M., Sundberg, L., Forsberg, A., Wolf-Watz, H., and Lloyd, S.A. (2003) YscP and YscU regulate substrate specificity of the *Yersinia* type III secretion system. *J Bacteriol* **185:** 2259–2266.
Espinosa, A., and Alfano, J.R. (2004) Disabling surveillance: bacterial type III secretion system effectors that suppress innate immunity. *Cell Microbiol* **6:** 1027–1040.
Ferracci, F., Schubot, F.D., Waugh, D.S., and Plano, G.V. (2005) Selection and characterization of *Yersinia pestis* YopN mutants that constitutively block Yop secretion. *Mol Microbiol* **57:** 970–987.
Forsberg, A., Viitanen, A.M., Skurnik, M., and Wolf-Watz, H. (1991) The surface-located YopN protein is involved in calcium signal transduction in *Yersinia pseudotuberculosis*. *Mol Microbiol* **5:** 977–986.
Gill, S.C., and von Hippel, P.H. (1989) Calculation of protein extinction coefficients from amino acid sequence data. *Anal Biochem* **182:** 319–326.
Heesemann, J., Gross, U., Schmidt, N., and Laufs, R. (1986) Immunochemical analysis of plasmid-encoded proteins released by enteropathogenic *Yersinia* sp. grown in calcium-deficient media. *Infect Immun* **54:** 561–567.
Joseph, S.S., and Plano, G.V. (2007) Identification of TyeA residues required to interact with YopN and to regulate Yop secretion. *Adv Exp Med Biol* **603:** 235–245.
Kenjale, R., Wilson, J., Zenk, S.F., Saurya, S., Picking, W.L., Picking, W.D., and Blocker, A. (2005) The needle component of the type III secreton of *Shigella* regulates the activity of the secretion apparatus. *J Biol Chem* **280:** 42929–42937.
Kimbrough, T.G., and Miller, S.I. (2002) Assembly of the type III secretion needle complex of *Salmonella typhimurium*. *Microbes Infect* **4:** 75–82.
Kotloff, K.L., Winickoff, J.P., Ivanoff, B., Clemens, J.D., Swerdlow, D.L., Sansonetti, P.J., *et al.* (1999) Global burden of *Shigella* infections: implications for vaccine development and implementation of control strategies. *Bull World Health Organ* **77:** 651–666.
Kubori, T., and Galan, J.E. (2002) *Salmonella* type III secretion-associated protein InvE controls translocation of effector proteins into host cells. *J Bacteriol* **184:** 4699–4708.
Kubori, T., Sukhan, A., Aizawa, S.I., and Galan, J.E. (2000) Molecular characterization and assembly of the needle complex of the *Salmonella typhimurium* type III protein secretion system. *Proc Natl Acad Sci USA* **97:** 10225–10230.
Lara-Tejero, M., Kato, J., Wagner, S., Liu, X., and Galan, J.E. (2011) A sorting platform determines the order of protein secretion in bacterial type III systems. *Science* **331:** 1188–1191.
Lorenz, C., and Buttner, D. (2011) Secretion of early and late substrates of the type III secretion system from *Xanthomonas* is controlled by HpaC and the C-terminal domain of HrcU. *Mol Microbiol* **79:** 447–467.
Lorenz, C., Schulz, S., Wolsch, T., Rossier, O., Bonas, U., and Buttner, D. (2008) HpaC controls substrate specificity

of the *Xanthomonas* type III secretion system. *PLoS Pathog* **4:** e1000094.
Magdalena, J., Hachani, A., Chamekh, M., Jouihri, N., Gounon, P., Blocker, A., and Allaoui, A. (2002) Spa32 regulates a switch in substrate specificity of the type III secreton of *Shigella flexneri* from needle components to Ipa proteins. *J Bacteriol* **184:** 3433–3441.
Marlovits, T.C., Kubori, T., Sukhan, A., Thomas, D.R., Galan, J.E., and Unger, V.M. (2004) Structural insights into the assembly of the type III secretion needle complex. *Science* **306:** 1040–1042.
Marlovits, T.C., Kubori, T., Lara-Tejero, M., Thomas, D., Unger, V.M., and Galan, J.E. (2006) Assembly of the inner rod determines needle length in the type III secretion injectisome. *Nature* **441:** 637–640.
Martinez, E., Bartolome, B., and de la Cruz, F. (1988) pACYC184-derived cloning vectors containing the multiple cloning site and *lacZ* alpha reporter gene of pUC8/9 and pUC18/19 plasmids. *Gene* **68:** 159–162.
Martinez-Argudo, I., and Blocker, A.J. (2010) The *Shigella* T3SS needle transmits a signal for MxiC release, which controls secretion of effectors. *Mol Microbiol* **78:** 1365–1378.
Mavris, M., Page, A.L., Tournebize, R., Demers, B., Sansonetti, P., and Parsot, C. (2002) Regulation of transcription by the activity of the *Shigella flexneri* type III secretion apparatus. *Mol Microbiol* **43:** 1543–1553.
Meitert, T., Pencu, E., Ciudin, L., Tonciu, M., Mihai, I., and Nicolescu, S. (1991) Correlation between Congo red binding as virulence marker in *Shigella* species and Sereny test. *Roum Arch Microbiol Immunol* **50:** 45–52.
Menard, R., Sansonetti, P.J., and Parsot, C. (1993) Nonpolar mutagenesis of the *ipa* genes defines IpaB, IpaC, and IpaD as effectors of *Shigella flexneri* entry into epithelial cells. *J Bacteriol* **175:** 5899–5906.
Menard, R., Sansonetti, P., and Parsot, C. (1994) The secretion of the *Shigella flexneri* Ipa invasins is activated by epithelial cells and controlled by IpaB and IpaD. *EMBO J* **13:** 5293–5302.
Ogawa, M., Handa, Y., Ashida, H., Suzuki, M., and Sasakawa, C. (2008) The versatility of *Shigella* effectors. *Nat Rev Microbiol* **6:** 11–16.
Olive, A.J., Kenjale, R., Espina, M., Moore, D.S., Picking, W.L., and Picking, W.D. (2007) Bile salts stimulate recruitment of IpaB to the *Shigella flexneri* surface, where it colocalizes with IpaD at the tip of the type III secretion needle. *Infect Immun* **75:** 2626–2629.
Page, A.L., Ohayon, H., Sansonetti, P.J., and Parsot, C. (1999) The secreted IpaB and IpaC invasins and their cytoplasmic chaperone IpgC are required for intercellular dissemination of *Shigella flexneri*. *Cell Microbiol* **1:** 183–193.
Pallen, M.J., Beatson, S.A., and Bailey, C.M. (2005) Bioinformatics analysis of the locus for enterocyte effacement provides novel insights into type-III secretion. *BMC Microbiol* **5:** 9.
Parsot, C. (2009) *Shigella* type III secretion effectors: how, where, when, for what purposes? *Curr Opin Microbiol* **12:** 110–116.
Parsot, C., Menard, R., Gounon, P., and Sansonetti, P.J. (1995) Enhanced secretion through the *Shigella flexneri* Mxi-Spa translocon leads to assembly of extracellular proteins into macromolecular structures. *Mol Microbiol* **16:** 291–300.
Parsot, C., Ageron, E., Penno, C., Mavris, M., Jamoussi, K., d'Hauteville, H., *et al*. (2005) A secreted anti-activator, OspD1, and its chaperone, Spa15, are involved in the control of transcription by the type III secretion apparatus activity in *Shigella flexneri*. *Mol Microbiol* **56:** 1627–1635.
Patel, J.C., and Galan, J.E. (2005) Manipulation of the host actin cytoskeleton by *Salmonella* – all in the name of entry. *Curr Opin Microbiol* **8:** 10–15.
Pilonieta, M.C., and Munson, G.P. (2008) The Chaperone IpgC copurifies with the virulence regulator MxiE. *J Bacteriol* **11:** 11.
Sal-Man, N., Deng, W., and Finlay, B.B. (2012) EscI: a crucial component of the type III secretion system forms the inner rod structure in enteropathogenic *Escherichia coli*. *Biochem J* **442:** 119–125.
Sarker, M.R., Neyt, C., Stainier, I., and Cornelis, G.R. (1998) The *Yersinia* Yop virulon: LcrV is required for extrusion of the translocators YopB and YopD. *J Bacteriol* **180:** 1207–1214.
Shao, F. (2008) Biochemical functions of *Yersinia* type III effectors. *Curr Opin Microbiol* **11:** 21–29.
Veenendaal, A.K., Hodgkinson, J.L., Schwarzer, L., Stabat, D., Zenk, S.F., and Blocker, A.J. (2007) The type III secretion system needle tip complex mediates host cell sensing and translocon insertion. *Mol Microbiol* **63:** 1719–1730.
Woestyn, S., Allaoui, A., Wattiau, P., and Cornelis, G.R. (1994) YscN, the putative energizer of the *Yersinia* Yop secretion machinery. *J Bacteriol* **176:** 1561–1569.
Wood, S.E., Jin, J., and Lloyd, S.A. (2008) YscP and YscU switch the substrate specificity of the *Yersinia* type III secretion system by regulating export of the inner rod protein YscI. *J Bacteriol* **190:** 4252–4262.

Supporting information

Additional supporting information may be found in the online version of this article.